

Efficient Median Filter Using Irregular Shape Window

Gou Chol Pok*

Abstract Median filtering is a nonlinear method which is known to be effective in removing impulse noise while preserving local image structure relatively well. However, it could still suffer the smearing phenomena of edges and fine details into neighbors due to undesirable influence from the pixels whose values are far off from the true value of the pixel at hand. This drawback mainly comes from the fact that median filters typically employ a regular shape window for collecting the pixels used in the filtering operation. In this paper, we propose a median filtering method which employs an irregular shape filter window in collecting neighboring pixels around the pixel to be denoised. By employing an irregular shape window, we can achieve good noise suppression while preserving image details. Experimental results have shown that our approach is superior to regular window-based methods.

Key Words : Denoising; image processing; impulse noise; irregular shape window; median filter

1. Introduction

Median filters have been well known to effectively remove impulse noise [1-3]. Although the median filter offers superior denoising performance, it tends to disrupt thin lines and to blur image details [4]. To address this problem, a lot of methods have been proposed in the literature. Weighted median filters [5-8] give different weights to pixels depending on the importance of the pixels. Switching median filters [9-11] first employ an impulse noise detector in order to determine whether the center pixel of a window is corrupted or not, and then median filtering operation is applied only to the pixels that are identified as noise. One of the advantages of the switching median filter is that median filtering is applied only to the corrupted pixels and hence undesirable filtering of clean pixels can be avoided. Adaptive median filters [12-14] use statistical

measures such as mean and variance and change the filter operation based on the statistical values in the window. It has been known that the performance of the adaptive filters is generally superior to non-adaptive filters, but the improvement comes at the cost of added filter complexity. Recently, soft-computing techniques such as fuzzy theory and support vector machine are combined with the median filtering [15]. It should be noted, however, that the soft-computing techniques generally require huge computing time and resources so that real time filtering is not feasible. Roy and Laskar [16] presented a linear prediction based adaptive filter to denoise color images. Noisy pixels are identified by comparing the linear prediction error with a predefined threshold, and adaptive vector median filtering is applied to the pixels with error greater than the threshold.

This work was supported by the research grant of Pai Chai University in 2018.

*Division of Computer and IT Education, Pai Chai University (gcpok@pcu.ac.kr)

Received August 23, 2018

Revised August 26, 2018

Accepted October 17, 2018

In this work, we assert that the local homogeneity property of images needs to be exploited to achieve the best denoising performance, and propose an improved median filtering method based on an irregular shape window which contains pixels with homogeneous values. The proposed method first identifies noise pixels under the local homogeneity level assumption, and then uses this information to determine the pixels to be denoised. If some pixels that are very close or even adjacent to the pixel to be denoised at hand are out of the homogeneity level of the noise pixel, then they are not included in the window and hence not in the denoising operation. In this manner our proposed method can achieve detail preservation by avoiding potentially undesirable effect from neighboring irrelevant pixels.

2. Methods

2.1 Identification of noisy pixels

We determine whether or not a pixel is corrupted by impulse noise based on the local homogeneity assumption around a pixel [17]. This noise identification process first collects the frequency of adjacent pixel values for each pixel value in the input image I . For this objective, we build a 2D histogram H of size 256×256 , where (i, j) -th element, $H(i, j)$, refers to the total number of neighboring pixels of value j around pixels of value i . Figure 1 shows the shape of H which resembles a half cylinder along the diagonal. The vertical cross-section of H at some point i on the x -axis denotes the cumulative distribution of pixel values neighboring to pixels of value i . For each pixel value i and a given percentage δ , we define the range of δ -homogeneity by two pixel values, $low\delta(i)$ and $up\delta(i)$, so that the sum of $H(i, j)$ with j running from $low\delta(i)$ to $up\delta(i)$ equals to δ percent of the sum of all the bins on the cross-section at i ,

$$\delta = 100 \frac{\sum_{j=low\delta}^{up\delta} H(i, j)}{\sum_{j=0}^{255} H(i, j)} \quad (1)$$

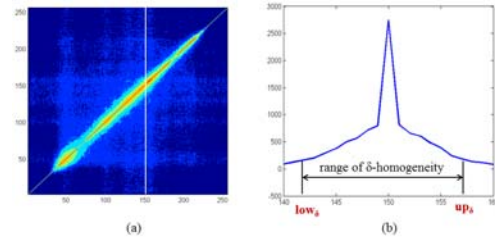


Fig. 1. (a) Color plot of histogram H for the Lena image. (b) Cross section of H at 150, which is the white line in (a).

Once values of $low\delta(i)$ and $up\delta(i)$ for all i have been computed, we determine if a pixel p is corrupted by noise according to the following criteria. For each of eight neighboring pixels that are adjacent to p , if p is in the range of the neighbor's δ -homogeneity, then the counter is increased by 1. After all the eight neighboring pixels are considered, if the counter is less than a threshold, which means that p is distinctive from the majority of its neighbors in terms of δ -homogeneity, then p is considered as noise and subject to subsequent denoising process.

2.2 Filtering by an Irregular Shape Window

Once the homogeneity levels for all the pixel values are determined and subsequently the locations of noise pixels are identified, the next step is to conduct the filtering operation in an irregular shape window. Here, the term "irregular" refers to that the shape of the analyzing window does not take the conventional $n \times n$ square type. The denoising operation is carried out as follows. First, the range of gra

y level intensities of the input image is divided into K sub-ranges of length L , $[0..L]$, $[L+1..2L]$, \dots , $[(K-1)L..255]$ where $K = 256/L$ and a binary image is built for each sub-range in such a way that if the gray level intensity of a pixel falls in the sub-range then the binary image takes value of 1 at the pixel and 0 otherwise.



Fig. 2. (a) Lena image with impulse noise rate of 30%, and the binary images with the white pixels belonging to (b) the intensity sub-range of $[60..80]$, (c) the sub-range of $[100..120]$, and (d) the sub-range of $[140..160]$.

Figure 2 shows the Lena image corrupted by impulse noise with rate of 30% and a number of binary images that are built by dividing the range of the intensities into 12 sub-ranges with length of 20. The binary images clearly represent the local image structures including the edges, lines, and fine details occurring in the corresponding sub-range of the intensities. The method proposed in this paper takes advantage of these properties that are captured in the binary images.

Figure 3(a) shows that the lower left part of Figure 2(b) is magnified to reveal clearly various local image structure. One can see a fine detail structure

in the eye area in Figure 3(b), an edge structure in Figure 3(c), and a line structure in Figure 3(d). In the figures, white pixels denote that their intensities belong to the sub-range of $[60..80]$, and the pixels marked by the symbol x are noisy pixels detected in the preprocessing step. In Figure 3(b), the upper noisy pixel is surrounded by six white pixels and the lower noisy pixel is surrounded by five white pixels. These six and five white pixels form the filtering window of the upper noisy pixel and the lower noisy pixel respectively. These filtering windows consist of different number of neighboring pixels with different shape as well. Figure 3(c) shows the cases where noisy pixels happen to be located adjacently. For these cases, two adjacent noisy pixels may be associated with the same filtering window having the same neighboring pixels. Figure 4 illustrates how the filtering windows are determined for two adjacent noisy pixels. In Figure 4(a), the filtering window contains three white pixels which are used for filtering of two noisy pixels. The intensity values of the white pixels are given on the right hand side. With these values the noisy pixels can be denoised by taking the median of the three values (67, 68, and 74), which is 68.

This median value of 68 may be used to replace both the noisy pixels marked by x . However, this naïve strategy of taking the median of neighboring pixels does not take into account the valuable information of adjacent pixel's intensity value. In other words, the upper noisy pixel is adjacent to the pixel with value of 68, whereas the lower noisy pixel is adjacent to the pixel with value of 74. This information is very useful for estimating the true value of the corrupted, noisy pixels adjacent to these pixels.

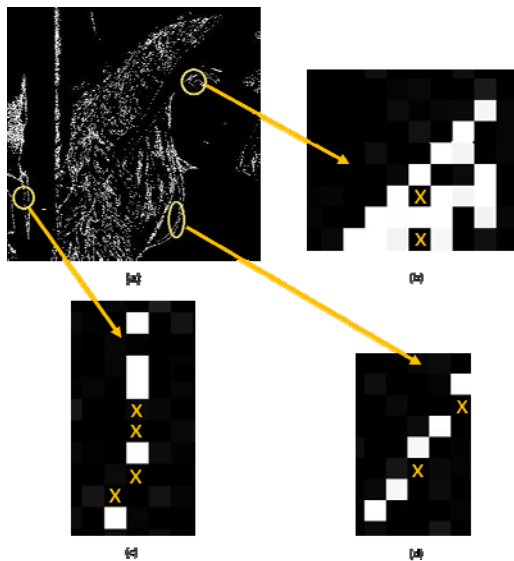


Fig. 3. Example of local image structures. (a) part of the binary image shown in Figure 2(b) above, (b) fine details in the eye area, (c) an edge structure, and (d) a line structure.

Therefore, instead of replacing both noisy pixels with the same median value of 68, we can use the values of the adjacent pixels by taking the mean of the median and the adjacent pixel's intensity value. Then, the upper noisy pixel is replaced with 68 which is computed by $(68+68) / 2$, and the lower noisy pixel is replaced with 71 which is computed by $(68 + 74) / 2$.

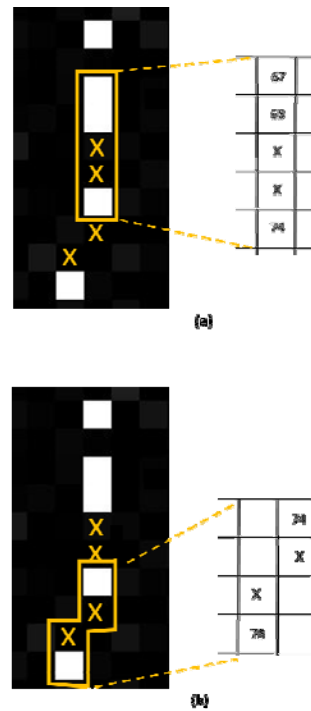


Fig. 4. Filtering window for (a) two adjacent noisy pixels surrounded by three white neighboring pixels, and (b) two adjacent noisy pixels surrounded by two white neighboring pixels.

Figure 4(b) shows another example of a line structure. In this case, there are two noisy pixels to be denoised, and there are also only two neighboring white pixels whose values are 74 and 78. For the two pixels, instead of computing the median, we compute the mean of two values, which is 76 by $(74 + 78) / 2$. Now, the noisy pixels are replaced with another mean of the mean above and the value of the adjacent pixel. For the upper noisy pixel within the window in Figure 4(b), the estimated value is 75 which is computed by $(76 + 74) / 2$, and the lower noisy pixel is replaced with 77 which is computed by $(76 + 78) / 2$. For the upper noisy pixel in Figure 3(d), denoising is performed by taking the median of the three white pixels surrounding the noisy pixel, and denoising of the lower noisy pixel

is performed by taking the median of the four white pixels surrounding it.

2.3 Algorithm to denoise impulse noise

The details of the proposed algorithm to denoise impulse noise can be summarized as follows in Algorithm 1.

Algorithm 1 Denoising by Irregular Shape Window

Input: noisy image I , Output: denoised image J ,
 Set the length of sub-ranges of the intensities to L ,
 Set $K = 255/L$,
 Define $W_p^{n \times n}$ to be an $n \times n$ square window over the center pixel p , not including p .

- 1 From I , build a 2D histogram H , and identify noisy pixels using the \mathcal{C} -homogeneity property.
- 2 From I , build binary images, B_0, B_1, \dots, B_{K-1} , such that the pixel values in $[ak \dots (a+1)k]$ are represented as 1 in B_a , and as 0 otherwise.
- 3 For a from 0 to $K-1$ do:
- 4 For each noisy pixel p in B_a do:
- 5 Define an irregular shape window
 $W_p = W_p^{3 \times 3} \cap B_a$
- 6 If W_p contains only one pixel, then do:
- 7 If p is the end of a line structure,
 then replace p 's value with the pixel value in W_p .
- 8 If p is adjacent to other noisy pixel,
 then expand W_p to $W_p = W_p^{7 \times 7} \cap B_a$
 and replace p 's value with the mean of p 's adjacent clean pixel and the median of pixels in expanded W_p .
- 9 If W_p contains only two pixels,
 then replace p 's value with the mean of pixel values in W_p .
- 11 If W_p contains more than two pixels,
 then replace p with the median of pixel values in W_p .
 Write the modified p 's value on J .
- 12 End for // of line 4
- 13 End for // of line 3
- 14 Write clean pixels in I on J .
- 15 End

3. Experimental Results

In order to evaluate the proposed method, we conducted a number of experiments using three images (Boat, Lena, Barbara image), with rate of 10%, 20%, and 30% impulse noise. Figure 5 shows the test images along with 30% noisy images.



Fig. 5. Test images (Boat, Lena, and Barbara from the left) and corresponding noisy images corrupted by 30% impulse noise

Table 1. Denoising results in PSNR (dB)

Image	Noise rate	Std. MF	TWW F	Proposed method		
				L=10	L=20	L=30
Boat	10%	30.5	35.1	35.2	37.1	36.1
	20%	27.8	30.2	31.9	34.3	32.3
	30%	27.9	29.5	30.4	32.7	29.5
Lena	10%	33.1	35.8	36.6	38.8	36.4
	20%	29.8	32.1	33.7	36.4	35.8
	30%	25.1	30.9	32.3	35.1	31.2
Barbara	10%	26.7	32.0	32.5	34.4	33.1
	20%	25.5	29.7	30.7	32.7	29.2
	30%	23.3	28.1	29.5	31.3	28.4

In the experiments, we varied the value of L from 10 to 30 to see the effect of the sub-range length. The denoising performance is measured by the peak signal-to-noise ratio (PSNR) which is defined as,

$$PSNR = 10 \cdot \log_{10} \left(\frac{MAX_I^2}{MSE} \right) \dots \dots (2)$$

where MAXI refers to the maximum possible pixel value of the image or 255 for the 8-bit image, and MSE stands for the mean square error which is defined as,

$$MSE = \frac{1}{mn} \sum_{i=0}^{m-1} \sum_{j=0}^{n-1} [J(i,j) - K(i,j)]^2 \quad (3)$$

where K is the ground truth image free of impulse noise and J is the output image which are denoised by the proposed algorithm.

Table I shows the experimental results for three methods, which are the standard median filter, the three valued weighted filter (TVWF) [7], and the proposed method for the test images with various noise rates. One can see that the proposed method outperforms other methods in terms of objective image quality.

Figure 6(a) shows an example of the denoised results of the Barbara image with 20% noise. Visual inspection of the denoised result indicate that fine details including stripes and patterns are well preserved. Figure 6(b) illustrates the locations where the denoising errors take place. The brighter the pixel is, the larger is the error magnitude. One can notice that most of the errors are occurring around the stripe patterns which can be easily influenced by neighboring pixels.

4. Conclusions

In this paper we presented an efficient denoising method for the images corrupted by impulse noise, which uses irregular shape windows based on the binary images constructed from intensity sub-ranges. As a preprocessing step, exact identification of the locations where noisy pixels are taking place is essential for good denoising performance. For this objective we introduced the concept of δ -homogeneity which indicates the range where the homoge-

neous property is preserved for each pixel. The identification of noisy pixel is performed by taking into account of the homogeneous levels for the neighboring pixels around the pixel at hand. Once all the noisy pixels are determined for the input image corrupted with impulse noise, the next step is to divide the range of pixel intensity values into K sub-ranges of length L, and then construct K binary images. By taking the intersection of the rectangular $n \times n$ window



Fig. 6. (a) Denoised results of the Barbara image with 20% noise. (b) The difference of between the clean image and the denoised image.

with the binary image, one can obtain an irregular shape window where the denoising operation is c

carried out. By employing irregular shape windows, the denoising operation can avoid the influence of the neighboring pixels that are irrelevant to the pixel to be denoised. Experiments with a number of test images have shown that the proposed method outperforms the conventional median filtering method.

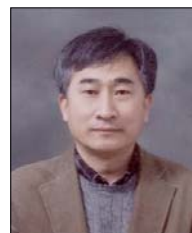
REFERENCES

- [1] J. Tukey, *Exploratory Data Analysis*. Addison-Wesley Menlo Park, CA, 1977.
- [2] T. Huang, G. Yang, and G. Tang, "A fast two-dimensional median filtering algorithm," *IEEE Trans. Acoust., Speech, Signal Processing*, vol. 27, no. 1, pp. 13-18, 1979.
- [3] J. Gil and M. Werman, "Computing 2-D Min, Median, and Max Filters," *IEEE Trans. Pattern Anal. Machine Intell.*, vol. 15, no. 5, pp. 504-507, 1993.
- [4] S. Vishaga, S. L. Das, "A survey on switching median filters for impulse noise removal," 2015 Int'l Conf. on Circuit, Power and Comp. Technologies, March 2015.
- [5] Lin Yin ; Ruikang Yang ; M. Gabbouj ; Y. Neuvuo, "Weighted median filters: a tutorial," *IEEE Trans. Circuits Systems II: Analog and Digital Sig. Processing*, vol. 43(2), pp. 157-192, 1996.
- [6] T. Chen, K.-K. Ma, L. Chen, "Tri-state median filter for image denoising," *IEEE Trans. Image Processing*, vol. 8, no. 12, pp. 1834-1838, 1999.
- [7] C. T. Lu, Y. Y. Chen, L.L. Wang, and C.F. Chang, "Removal of salt-and-pepper noise in corrupted image using three-values-weighted approach with variable-size window," *Pattern Recognition Letters*, vol.80, pp. 188-199, 2016.
- [8] S.-J. Ko, Y. H. Lee, "Center weighted median filters and their applications to image enhancement," *IEEE Trans. Circuits and Systems*, vol. 38, no. 9, pp. 984-993, 1991.
- [9] P. E. Ng, K. K. Ma, "A switching median filter with boundary discriminative noise detection for extremely corrupted images," *IEEE Trans. Image Processing*, vol.15, no. 6, pp. 1506-1516, 2006.
- [10] H.-L. Eng, K.-K. Ma, "Noise adaptive soft-switching median filter," *IEEE Trans. Image Processing*, vol.10, no. 2, pp. 242-251, 2001.
- [11] S. Zhang, M.A. Karim, "A new impulse detector for switching median filters," *IEEE Sig. Processing Letters*, vol. 9, no. 11, pp. 360-363, 2002.
- [12] T. Loupas, W. N. McDicken, P. L. Allan, "An adaptive weighted median filter for speckle suppression in medical ultrasonic images," *IEEE Trans. Circuits Systems*, vol. 36, no. 1, 1989.
- [13] H. Hwang, R. A. Haddad, "Adaptive median filters: new algorithms and results," *IEEE Trans. Image Processing*, vol. 4, no. 4, pp. 499-502, 1995.
- [14] T. C. Lin, P. T. Yu, "Adaptive two-pass median filter based on support vector machines for image restoration," *Neural Computation*, vol. 16, no. 2, pp. 332-353, 2004.
- [15] A. Roy, J. Singha, S.S. Devi, R.H. Laskar, "Impulse noise removal using SVM classification based fuzzy filter from gray scale images," *Signal Processing*, vol. 28, pp. 262-273, 2016.
- [16] A. Roy, R. H. Laskar, "Non-casual linear prediction based adaptive filter for removal of high density impulse noise from color images," *AEU - International Journal of Electronics and Communications* vol. 72, pp. 114-124, 2017.
- [17] G. Pok, J.-C. Liu, A.S. Nair, "Selective removal of impulse noise based on homogeneity level information," *IEEE Trans Image Processing*, vol. 12, no. 1, pp. 85-92, 2003.

Author Biography

Gou Chol Pok

[회원]



<Research
Interests>

- Aug. 1981 : Yonsei Univ., Mathematics, BS
 - Aug. 1995 : Texas A&M Univ., Computer Science, PhD
 - Feb. 2001 ~ Dec. 2010 : Yanbian University, Division of Computer Science
 - Mar. 2016 ~ current : PaiChai Univ., Jushikyung College
- Image processing,
Neural networks,
Pattern recognition